Processing and Application of Ceramics 10 [1] (2016) 1–8
DOI: 10.2298/PAC1601001P

Effect of particle size of starting materials on the structure and properties of biogenic hydroxyapatite/glass composites

Oleksandr Parkhomey, Nataliia Pinchuk, Olena Sych*, Tamara Tomila, Oleksiy Kuda, Hanna Tovstonoh, Viktor Gorban', Valeriy Kolesnichenko, Yan Evych

Frantsevich Institute for Problems of Materials Science of NAS of Ukraine, Department of Physical-Chemical Foundations of Powder Materials Technology, 3, Krzhyzhanovsky Str., Kyiv 03680, Ukraine

Received 22 October 2015; Received in revised form 23 January 2016; Accepted 8 February 2016

Abstract

The work is devoted to investigation of porous glass-ceramic composite materials on the basis of biogenic hydroxyapatite and sodium borosilicate glass prepared from starting powders with different particle sizes (<50 μm and <160 μm). Starting hydroxyapatite/glass weight ratio was 1.0/0.46 and sintering temperature was ~800 °C. Microstructural characterization of the surface and fracture of the samples revealed a decrease in sizes of grains and pores with decreasing the particle size of the precursor powder. However, porosity of the composites practically did not depend on the particle size and was equal to 32.5–33.0%. The same tendency was observed for the compression strength (66–67 MPa). However, investigation of structural-mechanical properties using an indentation method, where dominant load is applied to the surface layers of sample, showed up the effect of the particle size of the starting powder on the mechanical properties of the composites: the smaller particle size, the higher mechanical properties.

Keywords: *hydoxyapatite, glass ceramics, composites, structural characterization, mechanical properties*

I. Introduction

Studies in the field of development of medical materials for implants have taken a foreground position among the other scientific trends. In particular, hydroxyapatite $Ca_{10}(PO_4)_3(OH)_2$ is one of the most popular materials in the literature devoted to production and investigation of materials for reproduction of bone tissue.

Composites with glass take a particular place among the materials for osteoplasty. In order to fabricate composite materials on the basis of synthetic or biogenic hydroxyapatite (BHA), glass produced by both traditional melting and sol-gel method has been used alongside with industrial crushed glass [1–6]. Phosphate glass has been mostly used including the so-called Hench Bioglass®, aluminosilicate phosphate-free glass, and borosilicate glass (Borosil®, Pyrex®) [1,2,5,7–11].

Composites on the basis of commercial synthetic hydroxyapatite and commercial inert glass composites (5 and 10 wt.%) have been investigated and their mechanical properties were shown to decrease with increasing the glass content [12]. Hydroxyapatite composites based on hydroxyapatite produced from bovine bone with different weight percentage of soda-lime glass (0–5 wt.%) were obtained and demonstrated also a decrease in hardness and density with increasing additive glass content [13]. Belluccia *et al.* [14] have shown that mechanical properties of the composites with 80 wt.% bioglass and 20 wt.% HA are better than those of the reference Bioglass®45S5 samples. The reasons were the presence of HA, which is mechanically stronger than the 45S5 glass and the thermal behaviour of the modified bioglass are able to favour the sintering process of the composites. In addition, it was established that mechanical properties of BHA can be improved by the addition of 5 and 10 wt.% of bioglass and sintering at 1200–1300 °C for 4 h. In this study, the particle sizes of HA and bioglass were 106–150 μm and 100–130 μm, respectively. Moreover, the authors established the formation of new phases (tricalcium phosphate and various calcium silicates) due to the use of high sintering temperatures for composite production [6]. All similar papers mainly focus on the influence of sintering temperature and time as well as the composition of used glass.

*Corresponding author: tel: +38 066 112 25 25,
fax: +38 044 424 21 31, e-mail: *lena_sych@ukr.net*

There are no data on the effect of the starting powder size on the composite structure and mechanical properties.

Composite materials on the basis of biogenic hydroxyapatite (BHA) and sodium borosilicate (SBS) glass phase have been developed by our research team for a long time [15,16]. A number of the above-mentioned composite materials have been obtained and tested by colleagues in medicine, who demonstrated their successful application for treatment of defective bone tissue [17–19]. The authors have also produced and studied the properties of composite materials with hydroxyapatite/glass ratio close to 1.0/0.46 obtained by a two-stage sintering, which includes the use of glass-forming components [20]. Before-founded glass (ready glass) has not been used for production of composites of this composition, whereas it may markedly affect the structure and properties of composites.

The aim of this paper was to study the effect of the particle size of starting materials such as biogenic hydroxyapatite and ready sodium-borosilicate glass on the structure and properties of the composites produced.

II. Experimental

Hydroxyapatite/glass composite materials were produced using powders of biogenic hydroxyapatite (BHA) and sodium-borosilicate (SBS) glass. BHA was obtained according to the procedure described in Patent of Ukraine [21] and prepared with two different particle sizes, namely <50 μm and <160 μm. SBS glass (SiO_2 49.10 wt.%; Na_2O 28.14 wt.%; B_2O_3 22.76 wt.%) was produced by melting a mixture of the glass-forming components at 1100 °C for 1 h followed by cooling at room temperature. The glass was melted again at 1100 °C for 0.25 h and poured into water in order to obtain frit, which then was ground into powders with a particle size of <50 μm and <160 μm.

BHA/glass composites were produced by mixing SBS and BHA powders with a weight ratio of 0.46/1.0 and two different fractions, namely <50 μm (sample BHA/glass-50) and <160 μm (sample BHA/glass-160). Compact samples of ~3 g and ~15 mm in diameter were fabricated by half-dry pressing under pressure of 150 MPa and sintering at ~800 °C in air.

After sintering the samples were examined concerning the linear shrinkage along the diameter ($\Delta d/d_0$) and height ($\Delta h/h_0$), volume shrinkage ($\Delta V/V_0$), mass loss ($\Delta m/m_0$), apparent density (ρ) and total and open porosity (P_t and P_{op}). The structure of the composites was studied by scanning electron microscopy (SEM) using a microscope REM-106I (VAT SELMI, Ukraine) and analysed with the special material science complex program for analysis of structure images SIAMS-600 (SIAMS-Ltd, Russia). The phase composition was controlled by X-ray diffraction (XRD) analysis using a diffractometer Ultima IV (Rigaku, Japan). The starting powders were examined by differential thermal analysis (DTA) using "Derivatograph System" (MOM, Hungary) and heat rate of 10 °C/min. In addition, the materials were studied by infrared (IR) spectroscopy using a spectrophotometer FSM 1202 (TOV Infraspectr, Russia) in the wavenumber range 4000–400 cm^{-1}.

To specify mechanical properties such as Young's modulus (E), effective contact modulus of elasticity (E_r), hardness (H_{1T}), relative extra-contact elastic deformation (ε_{es}) and tension of extra-contact elastic deformation (σ_{es}), the method for automatic indentation of material [22,23] was used. The compression strength of samples (σ_p) was determined by a uniaxial compression using a universal machine Ceram test system (Ukraine).

Additionally, the properties of the obtained BHA/glass composites were compared with those of the composites obtained previously by two-stage sintering: in the first step the mixture of BHA powder and glass-forming components was sintered at 1100 °C and then the product was milled, sieved, uniaxially pressed to form disc-shaped samples and sintered at 800 °C [20].

III. Results and discussion

3.1. Structure

Figure 1 demonstrates XRD patterns of the starting BHA and SBS glass along with those for the composite materials made from the powders of different particle sizes. It can be seen that the obtained glass is amorphous and the starting BHA is crystalline with the pure $Ca_5(PO_4)_3(OH)$ phase (JCPDS No. 9-432). Upon sintering, the hydroxyapatite phase in the composites prepared from BHA and SBS glass at 800 °C was not changed, indicating that at the used sintering temperatures BHA is stable and does not react with the glass phase. No difference can be seen between the patterns of the composites obtained from the powders of different particle size (<50 μm and <160 μm). Thus, the particle size of the staring powders (PSSP) does not affect the composite phase composition.

These results were confirmed by DTA data (Fig. 2), which demonstrate the absence of phase transformation of the mixture composed of BHA and SBS glass up to 800 °C. It is well known that BHA is thermostable up to 1350 °C [24,25] and our glass does not tend towards liquation and crystallization after repeated heat treatment, so after sintering of the BHA/glass mixture phase transformations are not expected. As can be seen, the DT curve of the BHA/glass mixture and the basic line recorded for the standard Al_2O_3 sample of the same weight differ very slightly, by 0.5 °C, which is within the instrument inaccuracy. According to the TG curve, the mass loss of ~0.6% is related to the removal of absorbed water.

The results of IR spectroscopy for the starting materials and prepared composites are presented in Fig. 3. The IR spectrum of the starting BHA has characteristic bands of crystalline hydroxyapatite related to the vibrations of the main structural components such as

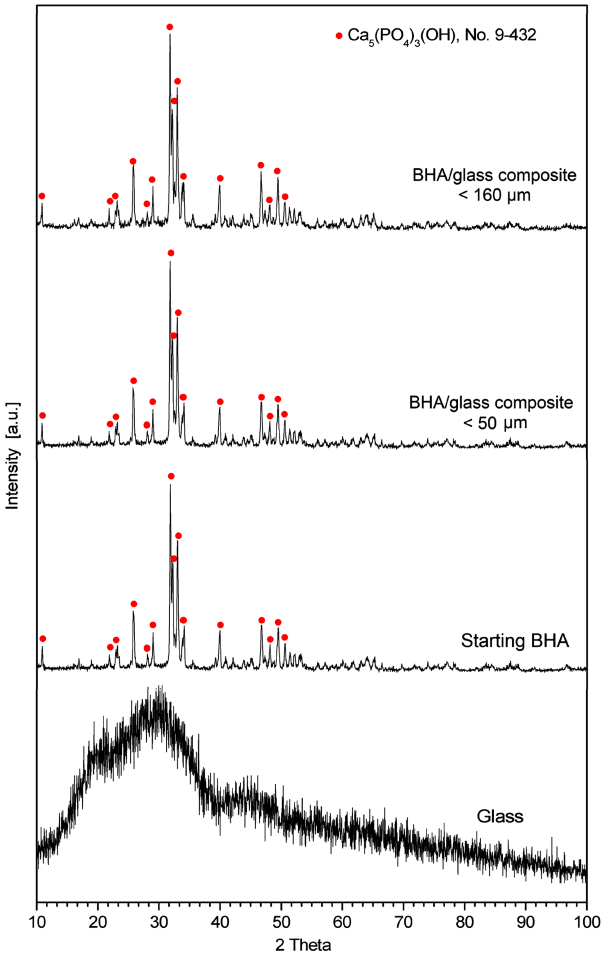

Figure 1. XRD patterns of starting materials and BHA/glass composites

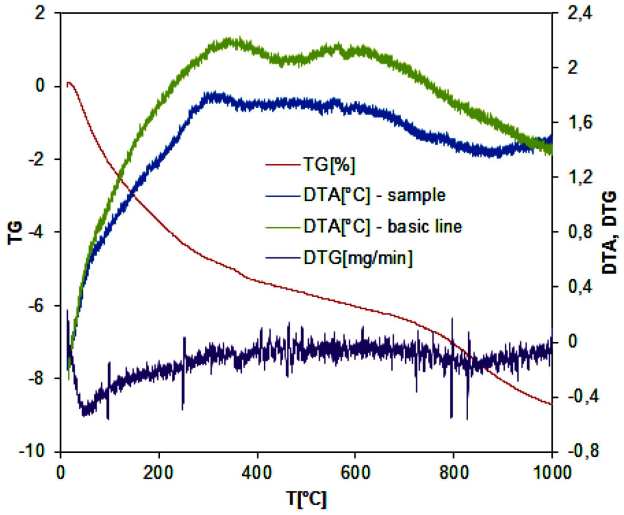

Figure 2. DTA results for BHA/glass charge

PO_4^{3-} (1090, 1050, 961, 604, 572, and 473 cm^{-1}) and OH^- (3574, 3440, 1630, 632 cm^{-1}). The spectrum also reflexes the vibrations of the carbonate group (1550, 1457, 1415, 880, and 800 cm^{-1}). Herein carbonate-ions in the BHA structure are in both A-site (replacing OH^- groups) and B-site (replacing PO_4^{3-} groups) [26,27]. The IR-spectrum of the starting SBS glass has broad absorption bands characteristic for amorphous materials (Fig. 1). The spectrum indicates the presence of asymmetric valence B–O vibrations in the trigonal coordination of boron (BO_3^-) in the range 1500–1400 cm^{-1} and deformation vibrations B–O–B at ~701 cm^{-1} [28,29]. There are also absorption bands in the region 1150–950 cm^{-1} associated with the Si–O–Si, B–O–B, and B–O–Si valence vibrations. The band at ~470 cm^{-1} corresponds to the Si–O–Si deformation vibrations. In addition, the spectrum contains bands of the OH^- group at ~3442 cm^{-1} and ~1635 cm^{-1}, which refer to valence and deformation vibrations, respectively.

The IR spectra of the composite materials obtained from the starting powders of different particle size (the samples BHA/glass-50 and BHA/glass-160) do not have any difference regarding to positions of the corresponding bands. A distinct feature of the IR spectrum of the composite BHA/glass-50 is higher intensities of absorption bands compared to those for the composite BHA/glass-160. The IR spectra of the composites contain bands which are characteristic for both the SBS glass and BHA in the form of superposition of their spectra. However, the absorption bands of the composites are somewhat wider, which evidences the presence of a glass phase. In the range 900–700 cm^{-1} new absorption bands appear: at ~849 cm^{-1} associated with the B–O vibrations, and at ~750 cm^{-1} and ~710 cm^{-1} associated with the P–O–P and B–O–B bonds, respectively. The following is also observed: i) the disappearance of the absorption band at 632 cm^{-1}, which corresponds to the liberation vibrations of OH^-; ii) changes in the band fine structure within 1550–1300 cm^{-1} and iii) the appearance of broad bands of middle intensity at 1460 and 1396 cm^{-1} shifted relative to the bands of both the starting SBS glass and BHA. The low-intensity bands in the range of 775–650 cm^{-1} may be associated with the vibrations characteristic for structures of the X_2O_7 (X = Si, P) type. However, according to the XRD data, there were neither pyrosilicates nor pyrophosphates, therefore the presence of these structural formations may only be suggested in small amount, not-detectable by XRD. Such changes in the IR spectrum relative to the spectra of the starting materials indicate the formation of composites on the basis of BHA and SBS glass.

In the IR spectra of the composites, absorption bands are observed at ~1460 cm^{-1} related to the carbonate CO_3^{2-} group. The formation of carbonates was not detected by XRD analysis, thus, one may suggest that amount of the formed CO_3^{2-} group is small and refers to the remaining starting components or to the functional groups absorbed on the surface. Because of overlapping IR absorption bands of BHA and SBS glass, it is difficult to precisely interpret the material composition.

After sintering, liner and volume shrinkage alongside with small mass loss are observed (Table 1). The mass loss for the composite BHA/glass-50 is somewhat greater than that for the composite BHA/glass-160, which may be attributed to more intense degassing

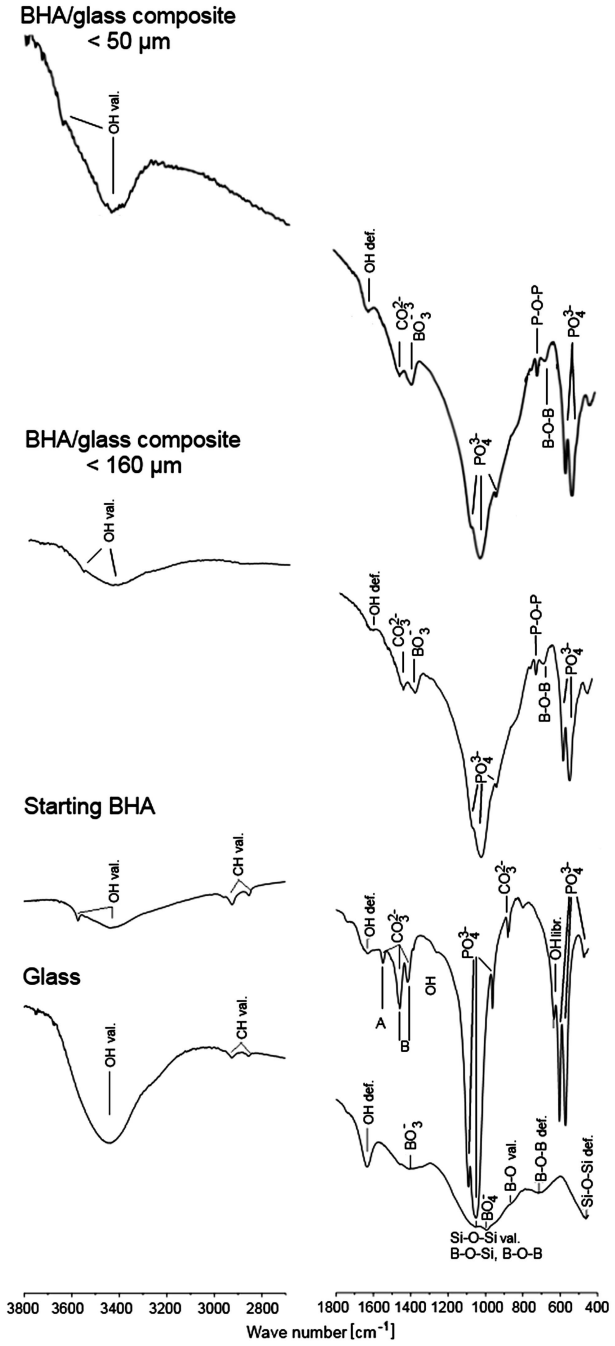

Figure 3. IR spectra of starting materials and BHA/glass composites

during sintering of the sample with a higher specific surface area, i.e. larger contact area. As for the shrinkage, its dependence on the PSSP is more evident, which is connected to sliding and shear of micrograins under liquid phase sintering [30]. The composites BHA/glass-160 undergo shrinkage along the height, whereas the samples BHA/glass-50 grows up, which may be prescribed to more intense processes under liquid phase sintering owing to the grain refinement in the crystalline phase. As a result of open and closed porosity transformations, accompanied by changes in the interpore spaces and resulted in redistribution of the gaseous phase and partial degassing, when the glass phase viscosity remains high enough to retard these processes, slight foaming may occur, which leads to increasing the sample height. In addition, the diameter of sample changes as well due to the crystalline phase densification: shrinkage is greater for the composites BHA/glass-160 as compared to that for the composite BHA/glass-50. Herein the overall changes throughout the volume of sample include shrinkage of both types and come to 1.62% shrinkage for the composites prepared from the powders with PSSP <160 μm and slight grows (0.27%) for the composites BHA/glass-50. Moreover, it should be noticed that the volume shrinkage of the composites prepared from the powders with PSSP <160 μm sintered with the ready glass is lower than that of the composites prepared by two-stage sintering (Table 1).

Microstructures of the composites obtained from the powders with different PSSP (Fig. 4) display substantial difference between the surface and fracture of the samples: the surface is less porous. This may be related to its vitrification, as at sintering temperature of 800 °C the glass mass is in a viscous-flow state and practically completely wets crystalline BHA particles, which alongside with surface tension forces promotes the formation of a vitrified surface. During melting, glass mass is known to absorb a large amount of gases which are released under repeated heating, and at 800 °C viscosity of glass mass still remains high enough for complete removal of gaseous products. As a result of the above described sintering processes, an irregular porous microstructure is formed not only in the volume but also on the surface. This can be confirmed by the pore size distribution of the materials (Fig. 5, Table 2). Also, a distinct difference in the composite porous structure can be noticed for different PSSP. Pore size at the surface and fracture of the samples is smaller for the material BHA/glass-50. Investigation of pore size distribution over the surface of the composites made from the powder with PSSP <50 μm revealed the dominance of small 0.4–5.0 μm pores (88%). Furthermore, on the compos-

Table 1. Sintering parameters of BHA/glass samples

Sample	Sintering conditions	Shrinkage			
		$\Delta m/m$ ±0.1%	$\Delta h/h$ ±0.04%	$\Delta d/d$ ±0.04%	$\Delta V/V$ ±0.075%
BHA/glass-50	one-stage (800 °C)	0.5	-0.77	0.3	-0.27
BHA/glass-160	one-stage (800 °C)	0.4	0.41	0.51	1.62
BHA/glass-160	two-stage (1100 °C and 800 °C)	0.2[a]	1.03[a]	0.65[a]	2.32[a]

[a] Results presented in ref [20]

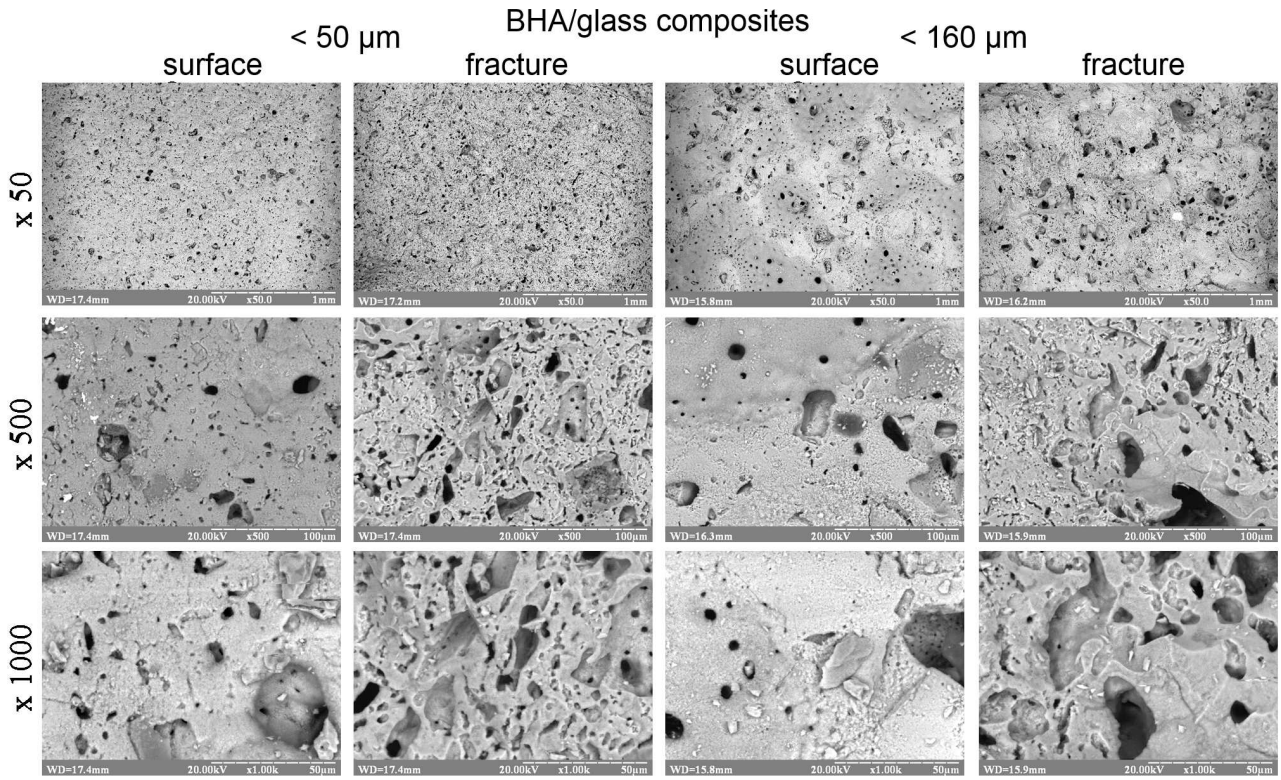

Figure 4. SEM results for BHA/glass composites

ite surface ~9% of pores are in the range 5–10 μm and the rest of them are over 10 μm (maximal size 98 μm). Inside the sample the number of 0.8–5.0 μm pores decreases down to 73%, whereas the number of 5–10 μm pores increases up to ~18%. The rest of the pores are larger than 10 μm and the biggest have size even above 100 μm (Table 2, Fig. 5).

The surface structure of the composite materials obtained from the powder with PSSP <160 μm is characterized by broadening of the region of pores with dominant sizes: about 52% pores have sizes within 1.5–5.0 μm, ~28% pores within 5–10 μm, ~6% within 10–15 μm, and ~5% within 15–20 μm, etc. (Fig. 5). Inside the sample BHA/glass-160 practically all of the pores (~95%) have sizes 1–10 μm, only 3% 10–20 μm, and the rest of them are over 20 μm up to the maximal size of 152 μm.

The total porosity of the obtained composites does not depend on the particle size of the staring powders (PSSP) and is equal to 32.5–33.0%, whereas the samples of the same composition obtained by two-stage sintering had a porosity of 25.5% (Table 3). Moreover, the examination of microstructure revealed that it is difficult to discern individual particles in composite structure because of vitrification of samples both on the surface and in the volume (Fig. 4).

3.2. Mechanical properties

It has been established before [22,23] that load diagrams obtained by an automatic indentation method according to the international standard ISO14577-1:2002(E) are informative enough concerning all of the basic mechanical properties of samples. Herein the relationship between the diagram parameters and the structural characteristics of material is related to the relationship between hardness and modulus of elasticity (H_{1T}/E_r). The use of these procedures of processing and analysis of automatic indentation results makes it possible to determine not only mechanical properties of materials but also their structural state.

Mechanical properties of the composites calculated using diagrams of automatic indentation are presented in Table 3. In general, all of the obtained mechanical characteristics such as Young's modulus, effective

Table 2. Research results of porous structure of BHA/glass samples

	Starting particle size <50 μm		Starting particle size <160 μm	
	surface	fracture	surface	fracture
Minimal size [μm]	0.40	0.80	1.50	1.00
Maximal size [μm]	97.90	102.40	113.10	152.20
Average size [μm]	3.00	4.60	9.2	4.70
Standard deviation [μm]	4.45	5.94	11.44	8.36
Variation coefficient	1.48	1.29	1.24	1.83

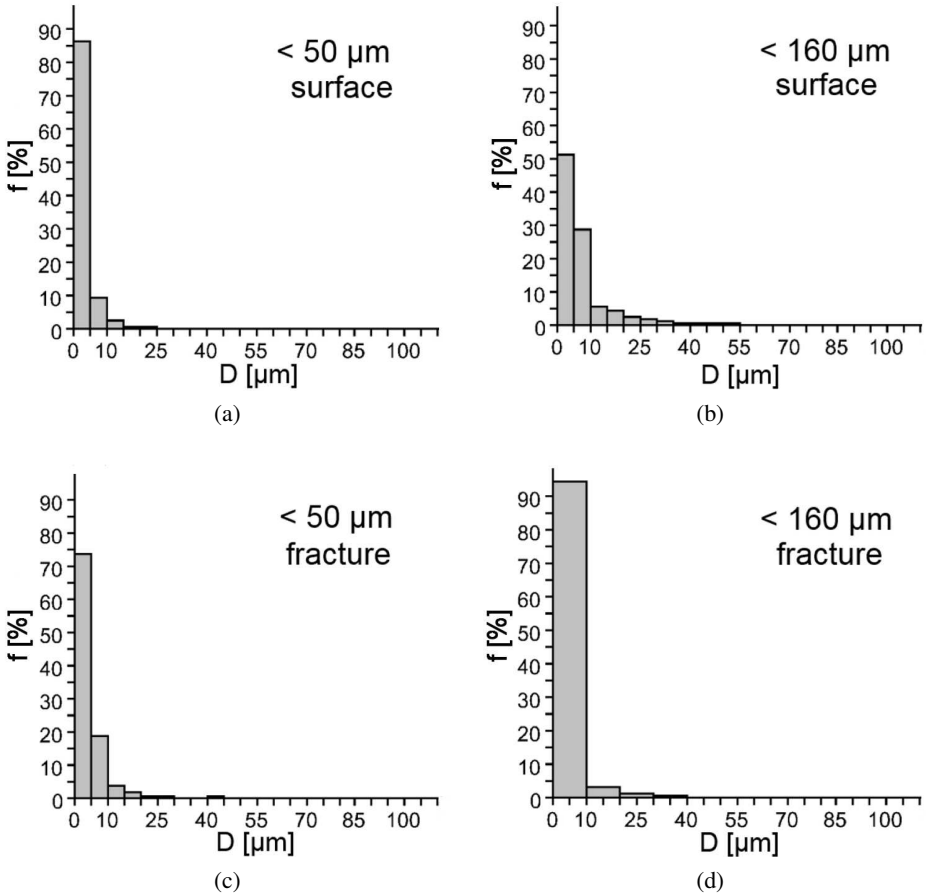

Figure 5. Pore size distribution in structure of BHA/glass composites

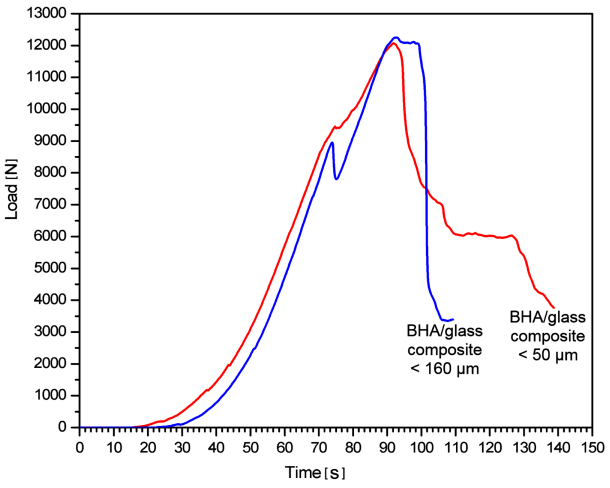

Figure 6. Typical loading diagram for BHA/glass composites

contact modulus of elasticity, hardness, relative extra-contact elastic deformation, tension of extra-contact elastic deformation are higher for composites produced from the powders with PSSP <50 μm than the corresponding characteristics of composites obtained from powders with PSSP <160 μm. These physicomechanical properties make it possible to establish the material structural state, in particular to conclude that the obtained composites refer to materials with coarse or fine crystalline structure depending on PSSP. Some parameters, namely the level of strengthening ($H_{1T}/E > 0.05$) and elastic deformation ε_{es} (1.3–3.0%), for the obtained composites BHA/glass-50, indicate nanostructural state of material, in particular for the surface layers of the samples. Thanks to the small PSSP, upon sintering in the presence of liquid glass phase, strengthening occurs at the expense of formation of a condensation-crystallized structure in the system "crystalline phase – amorphous state" [31].

Figure 6 shows loading diagrams for the composite samples. Both types are characterized by brittle fracture, which is typical for glass ceramics. However, the samples made from the finer fraction resist fracturing for a longer time. The compression strength does not depend on PSSP (Table 3) and is close to that of native bone tissue [32].

Some differences can be noticed between characteristics obtained by using an indentation method and uniaxial compression: the indentation-determined mechanical properties depend on PSSP: the smaller PSSP, the higher structural-mechanical properties of the composite material. This may be related to the fact that in the former case, dominant load is applied to the surface layers of the material which can be vitrified and thus less porous, whereas in the latter case, all the volume is affected. Moreover, it is known that mineral fillers (in

Table 3. Properties of BHA/glass samples

Sample	Sintering conditions	$\rho_{aparent}$ [g/cm^3]	Porosity [%] total	open	$\sigma_{comp.}$ [MPa]	H_{1T} [GPa]	E_r [GPa]	H_{1T}/E_r	σ_{el} [GPa]
BHA/glass-50	one-stage (800 °C)	1.89	33.0	2.6	66	1.70	27	0.065	0.52
BHA/glass-160	one-stage (800 °C)	1.91	32.5	4.5	67	0.63	23	0.027	0.19
BHA/glass-160	two-stage (1100 °C and 800 °C)	2.12[a]	25.5[a]	–	75[a]	0.70[a]	35[a]	0.020[a]	0.22[a]

[a] Results presented in ref [20]

this case BHA) increase rigidity of material and a decrease in their particle size results in increasing elastic deformation of composite materials [31]. In our case, the relationship between the matrix (SBS glass) and the filler (BHA) in composites provides the dominance of the matrix on the surface of the samples after sintering, which results in obtaining an anisotropic material with non-additive properties.

IV. Conclusions

Hydroxyapatite/glass composite materials were prepared using powders of biogenic hydroxyapatite (BHA) and sodium-borosilicate (SBS) glass with different particle sizes (<50 μm and <160 μm). The effect of the particle size of the staring powders (PSSP) on the structure and mechanical properties of the composite materials was investigated. It was shown that the structure of both surface and fracture is characterized by decreasing pore size with decreasing PSSP. Practically, the total porosity of composite does not depend on PSSP and is 32.5–33.0%. The same tendency was observed for the compression strength, which equals 66–67 MPa. Additionally, investigation of mechanical properties using the indention method revealed their dependence on PSSP. In particular, the composites obtained from the powder with PSSP <50 μm exhibit better mechanical properties compared to those obtained from the powder with PSSP of <160 μm.

Acknowledgements: The authors would like to express their sincere thanks to Dr. L. Ivanchenko for her assistance in planning the experiment.

References

1. K. So, S. Fujibayashi, M. Neo, Y. Anan, T. Ogawa, T. Kokubo, T. Nakamura, "Accelerated degradation and improved bone-bonding ability of hydroxyapatite ceramics by the addition of glass", *Biomater.*, **27** [7] (2006) 4738–4744.
2. S. Callcut, J.C. Knowles, "Correlation between structure and compressive strength in a reticulated glass-reinforced hyaroxyapatite foam", *J. Mater. Sci.: Mater. Med.*, **13** (2002) 485–489.
3. G. Goller, F.N. Oktar, H. Demirkiran, E. Demirkesen, "Effects on mechanical properties of bioglass reinforced hydroxyapatite composites", *Key Eng. Mater.*, **240-242** (2003) 939–942.
4. R. Ravarian, F. Moztarzadeh, M. Solati Hashjin, S.M. Rabiee, P. Khoshakhlagh, M. Tahriri, "Synthesis, characterization and bioactivity investigation of bioglass/hydroxyapatite composite", *Ceram. Int.*, **36** [1] (2010) 291–297.
5. C.P. Yoganand, V. Selvarajan, J. Wu, D. Xue, "Processing of bovine hydroxyapatite (HA) powders and synthesis of calcium phosphate silicate glass ceramics using DC thermal plasma torch", *Vacuum*, **83** [2] (2009) 319–325.
6. S. Salman, F.N. Oktar, O. Gunduz, S. Agathopoulos, M.L. Öveçoğlu, E.S. Kayali, "Sintering effect on mechanical properties of composites made of bovine hydroxyapatite (BHA) and commercial inert glass (CIG)", *Key Eng. Mater.*, **330-332** (2007) 189–192.
7. M.A. Lopes, F.J. Monteiro, J.H.D. Santos, "Glass-reinforced hydroxyapatite composites: fracture toughness and hardness dependence on microstructural characteristics", *Biomater.*, **20** [21] (1999) 2085–2090.
8. L.-H. He, O.C. Standard, T.T.Y. Huang, B.A. Latella, M.V. Swain, "Mechanical behaviour of porous hydroxyapatite", *Acta Biomater.*, **4** [3] (2008) 577–586.
9. A. Yao, F. Ai, X. Liu, D. Wang, W. Huang, W. Xu, "Preparation of hollow hydroxyapatite microspheres by the conversion of borate glass at near room temperature", *Mater. Res. Bull.*, **45** [1] (2010) 25–28.
10. A.Yu. Malysheva, B.I. Beletskii, E.B. Vlasova, "Structure and properties of composite materials for medical application", *Glass Ceram.*, **58** [1-2] (2001) 66–69.
11. D.L. Mastryukova, B.I. Beletskii, O.V. Polukhina, "Glass ceramics with controllable pore structure for medicine", *Glass Ceram.*, **64** [3-4] (2007) 132–135.
12. N. Demirkol, F.N. Oktar, E.S. Kayali, "Influence of commercial inert glass addition on the mechanical properties of commercial synthetic hydroxyapatite", *Acta. Phys. Pol. A*, **123** [2] (2013) 427–429.
13. Z. Yazdanpanah, M.E. Bahrololoom, B. Hashemi, "Evaluating morphology and mechanical properties of glass-reinforced natural hydroxyapatite composites", *J. Mech. Behav. Biomed. Mater.*, **41** (2015) 36–42.
14. D. Belluccia, A. Solaa, A. Anesib, R. Salvatorib, L. Chiarinib, V. Cannilloa. "Bioactive glass/hydroxyapatite composites: Mechanical properties and biological evaluation", *Mater. Sci. Eng. C*, **51** (2015) 196–205.
15. L.A. Ivanchenko, T.I. Fal'kovskaya, N.D. Pinchuk, O.V. Lavrent'eva, I.A. Lagunova, "Preparation and

properties of hydroxyapatite strengthened with a glass phase", *Powder Metall. Met. Ceram.*, **42** [1-2] (2003) 54–59.
16. N.D. Pinchuk, L.A. Ivachenko, "Making calcium phosphate biomaterials", *Powder Metall. Met. Ceram.*, **42** [7-8] (2003) 357–371.
17. L.A. Ivanchenko, A.R. Parkhomei, A.G. Popandopulo, A.V. Oberemko, "Possibilities of using composite hydroxyapatite ceramics as carriers of cultured stem cells", *Glass Ceram.*, **68** [11-12] (2012) 378–381.
18. V. Luzin, D. Astrakhantsev, M. Solyanaya, V. Morozov, "Effects of biogenic hydroxyapatite implants on growth and formation of mandible in rats", *Bone*, **46** [1] (2010) S74.
19. A. Lubenets, V. Luzin, V. Stry, D. Astrakhantsev, R. Vereskun, "The ultrastructure of hip bone mineral after implantations into tibia biological hydroxyapatite saturated by salt of different metals", *Bone*, **48** [2] (2011) S171.
20. L.A. Ivanchenko, N.D. Pinchuk, A.R. Parkhomei, M.E. Golovkova, M.I. Molchanovskaya, A.N. Syabro, "Effect of cerium dioxide on the properties of biogenic hydroxyapatite sintered with borosilicate glass", *Powder Metall. Met. Ceram.*, **48** [5-6] (2009) 305–310.
21. Y.P. Podrushniak, L.A. Ivanchenko, V.L. Ivanchenko, N.D. Pinchuk, "Hydroxyapatite and method of its manufacturing (versions)", *UA patent 61938* December, 2003.
22. V.F. Gorban', É.P. Pechkovski, "Instrumented indentation for determining the structural state of materials", *Powder Metall. Met. Ceram.*, **49** [7] (2010) 424–429.
23. S.A. Firstov, V.F. Gorban', É.P. Pechkovski, N.A. Mameka, "The relationship strength characteristics of materials with parameters instrumented indentation", *Mater. Sci.*, **11** (2007) 26–31.
24. F.N. Oktar, "Microstructure and mechanical properties of sintered enamel hydroxyapatite", *Ceram. Int.*, **33** [7] (2007) 1309–1314.
25. G. Gergely, F. Wéber, I. Lukács, A.L. Tóth, Z.E. Horváth, J. Mihály, C. Balázsi, "Preparation and characterization of hydroxyapatite from eggshell", *Ceram. Int.*, **36** [2] (2010) 803–806.
26. E.E. Sych, N.D. Pinchuk, V.P. Klimenko, I.V. Uvarova, A.B. Tovstonog, T.V. Tomila, Ya.I. Evich, "Synthesis and properties of Si-modified biogenic hydroxyapatite ceramics", *Powder Metall. Met. Ceram.*, **54** [1-2] (2015) 67–73.
27. E.E. Sych, "Effect of pyrogenic silicon dioxide on the structure and properties of hydroxyapatite based bioceramics", *Glass Ceram.*, **72** [3-4] (2015) 107–110.
28. M.A. Ouis, A.M. Abdelghany, H.A. ElBatal, "Corrosion mechanism and bioactivity of borate glasses analogue to Hench's bioglass", *Process. Appl. Ceram.*, **6** [3] (2012) 141–149.
29. C. Gautam, A.K. Yadav, A.K. Singh, "Review on infrared spectroscopy of borate glasses with effects of different additives", *ISRN Ceramics*, **2012** (2012) 428497 (17 pages).
30. S. Somiya, *Handbook of Advanced Ceramics*, Elsevier Inc., 2003.
31. Y.G. Frolov, *Course of Colloid Chemistry (Surface Phenomena and Disperse Systems) - Textbook for High Schools*, Chemistry, Moscow, 1982.
32. S.A. Goldstein, "The mechanical properties of trabecular bone: dependence on anatomic location and function", *J. Biomech.*, **20** [11-12] (1987) 1055–1061.